Particle Accelerators, 1996, Vol. 52, pp. 179–200
Reprints available directly from the publisher
Photocopying permitted by license only

THE COUPLING IMPEDANCE OF PERIODIC IRISES IN A BEAM PIPE*

SHICHENG JIANG,[1] ROBERT L. GLUCKSTERN[1] and HIROMI OKAMOTO[2]

[1] *Physics Department, University of Maryland, College Park, Maryland 20742, USA*

[2] *Institute for Chemical Research, Kyoto University, Kyoto 611, Japan*

(Received 4 August 1995; in final form 31 January 1996)

In a recent paper,[1] we constructed a variational form to calculate both the longitudinal and transverse impedance of a thick iris in a beam pipe for a point charge at ultrarelativistic velocity in a lossless geometry. Implementation of this calculation led to rapidly converging and accurate values for these impedances for a circular beam pipe and iris. We have now constructed an analogous variational form for the longitudinal and transverse impedance of periodic irises in a beam pipe, with similar convergence and accuracy properties. In this case the numerically calculated impedance is imaginary, except for isolated narrow resonances corresponding to modes propagating with the velocity of light. The real part of impedance is obtained by using causality. Analytical and numerical results are presented and discussed.

Keywords: Electromagnetic field calculations, impedances

1 INTRODUCTION

In a previous publication,[1] we calculated both the longitudinal and transverse coupling impedance of an iris in a beam pipe. In particular we constructed a variational formulation for the impedance, where the trial function was the transverse electric fields at the two junctions of the beam pipe and the iris. The numerical implementation of this formulation proved to be extremely well convergent, requiring only a few terms in the expansion of the trial functions in terms of TM and TE transverse modes in the iris region. Although the formulation worked for all values of the parameters (pipe radius, wavelength, iris radius and iris thickness) the primary region studied numerically was the limit of large pipe radius, eventually providing information about the impedance of a circular hole in a thick plate, which had been studied earlier.[2]

*Work supported by the U.S. Department of Energy.

In this work we construct a corresponding variational formulation for the longitudinal and transverse impedance of periodic irises in a beam pipe. Once again the numerical implementation is well convergent. We present these results in Sections 5 for a point charge at ultrarelativistic velocity in a lossless geometry. The results are similar to those of Keil and Zotter,[3,4] who used finite beam dimensions, finite wall conductivity. Equations have also been obtained by Dôme etc.[5] for the longitudinal impedance of a periodic array of thin plates with a circular hole for finite γ, but they give no numerical results with which we can compare.

In Section 2 we present a general analysis for the fields, leading to the integral equations for the unknown transverse electric fields, and in Section 3 we construct a variational form for the impedance integrals.

Section 4 contains some general observations about the form of the real and imaginary parts of the impedances. The numerical implementation for circular irises in a cylindrical beam pipe is presented in Section 5 for the longitudinal and transverse impedances.

2 GENERAL ANALYSIS

We will consider a beam pipe of arbitrary cross section loaded with periodic irises of arbitrary cross section, both homogeneous in the axial direction. The planes involving the iris side walls are perpendicular to the beam pipe axis. We denote the period of the irises as L, and the width of the irises as g. We consider the m$^{\text{th}}$ iris and its following pipe cavity as the cell, whose length is L. We set the coordinate origin at the center of the zeroth iris and the axis of the pipe as the z coordinate. The cross-sectional area of the iris hole is denoted by S_1 while S_2 represents the side walls of the iris. In the following we will derive the electromagnetic fields in the iris hole and the pipe cavity of the cell respectively.

Both in the iris hole and in the pipe cavity, the electromagnetic fields are superpositions of source fields and pipe fields which can be expanded as sums over the normal modes in relevant regions. We use Latin letters as the subscripts of the quantities defined in the pipe cavity, and Greek letters for those defined in the iris hole. The time dependent factor $\exp(j\omega t)$ attached to all fields is omitted in the following for simplicity.

2.1 Fields in the Pipe Cavity

In the pipe cavity region, the source fields are generated by the ultrarelativistic charged particle beam moving near or along the axis of smooth pipe without irises loading. The pipe is perfectly conducting and therefore the fields are transverse.

Thus, the source fields can be written as

$$\mathbf{E}_0 = Z_0\mathbf{H}_0 \times \hat{\mathbf{z}} = A_0 e^{-jkz}\nabla\chi(\mathbf{r}), \tag{1}$$

where Z_0 is the free-space impedance, A_0 is a constant, and $\hat{\mathbf{z}}$ is unit vector in positive z direction. We define ∇ as

$$\nabla = \hat{\mathbf{x}}\frac{\partial}{\partial x} + \hat{\mathbf{y}}\frac{\partial}{\partial y}. \tag{2}$$

The source field potential $\chi(\mathbf{r})$ is a function of transverse coordinates $\mathbf{r} = (x, y)$ or (r, θ) and it must satisfy the proper boundary condition on the pipe surface. The forms of A_0 and χ depend on which impedance we consider, i.e., longitudinal monopole impedance or transverse dipole impedance.

The normal modes of electromagnetic fields (including both TM and TE modes) in the pipe cavity are transverse and normalized on the cross section of the pipe $S_1 + S_2$. For the electric field, the n$^{\text{th}}$ mode is written as $\mathbf{e}_n$, which is a function of transverse coordinates x and y only, satisfying

$$\int_{S_1+S_2} \mathbf{e}_n \cdot \mathbf{e}_{n'} dS = \delta_{nn'}. \tag{3}$$

The corresponding normal mode for the magnetic field is represented as

$$\mathbf{h}_n = \hat{\mathbf{z}} \times \mathbf{e}_n. \tag{4}$$

The pipe fields contain waves traveling both to the left and right with wave number β_n. Floquet's theorem says that in a periodic structure the electromagnetic fields in the (m+1)$^{\text{th}}$ cell must be identical to those in the m$^{\text{th}}$ cell except for a constant phase factor e^{-jkL}, set by the charge traveling with velocity c. By applying Floquet's theorem, we write the transverse total fields $\mathbf{E}_\perp$ and $\mathbf{H}_\perp$ as

$$\frac{\mathbf{E}_\perp}{A_0} = e^{-jkz}\nabla\chi + \sum_n \mathbf{e}_n e^{-jkmL}[A_n e^{-j\beta_n(z-mL)} + B_n e^{j\beta_n(z-mL)}], \tag{5}$$

$$\frac{Z_0\mathbf{H}_\perp \times \hat{\mathbf{z}}}{A_0} = e^{-jkz}\nabla\chi + \sum_n \mathbf{e}_n\lambda_n e^{-jkmL}[A_n e^{-j\beta_n(z-mL)} - B_n e^{j\beta_n(z-mL)}]. \tag{6}$$

Here, A_n and B_n are expansion coefficients for the right and left traveling waves respectively and λ_n is k/β_n for TM modes, β_n/k for TE modes.

2.2 Fields in the Iris Hole

In the iris hole, the source field potential is replaced by $\sigma(\mathbf{r})$ which satisfies the boundary condition on the hole surface. The μ^{th} normal mode of the electric field inside the iris hole is defined on the hole cross section S_1 as

$$\int_{S_1} \mathbf{e}_\mu \cdot \mathbf{e}_{\mu'} dS = \delta_{\mu\mu'}, \tag{7}$$

and the corresponding normal mode of the magnetic field is $\mathbf{h}_\mu = \hat{\mathbf{z}} \times \mathbf{e}_\mu$. The transverse total fields in this region are

$$\frac{\mathbf{E}_\perp}{A_0} = e^{-jkz}\nabla\sigma + \sum_\mu \mathbf{e}_\mu e^{-jkmL}[C_\mu e^{-j\beta_\mu(z-mL)} + D_\mu e^{j\beta_\mu(z-mL)}], \tag{8}$$

$$\frac{Z_0\mathbf{H}_\perp \times \hat{\mathbf{z}}}{A_0} = e^{-jkz}\nabla\sigma + \sum_\mu \mathbf{e}_\mu \lambda_\mu e^{-jkmL}[C_\mu e^{-j\beta_\mu(z-mL)} + D_\mu e^{j\beta_\mu(z-mL)}]. \tag{9}$$

Here, C_μ and D_μ are expansion coefficients, λ_μ is k/β_μ for TM modes and β_μ/k for TE modes, and β_μ is the wave number in the iris hole.

2.3 Field Matching

We will match the transverse electromagnetic fields at $z = mL + g/2$ and $z = mL - g/2$. For convenience in the derivation, we introduce two transverse electric fields $\mathbf{u}(\mathbf{r})$ and $\mathbf{v}(\mathbf{r})$ which are defined at $z = mL + g/2$ and $z = mL - g/2$ respectively.

$$\frac{\mathbf{E}_\perp}{A_0} = \begin{cases} (\mathbf{u} + \nabla\sigma)e^{-jk(mL+\frac{g}{2})} \text{ on } S_1, \\ 0 \text{ on } S_2 \end{cases} \quad \text{at } z = mL + \frac{g}{2}; \tag{10}$$

$$\frac{\mathbf{E}_\perp}{A_0} = \begin{cases} (\mathbf{v} + \nabla\sigma)e^{-jk(mL-\frac{g}{2})} \text{ on } S_1, \\ 0 \text{ on } S_2 \end{cases} \quad \text{at } z = mL - \frac{g}{2}. \tag{11}$$

Let the right hand side (RHS) of Equation (5) be equal to the RHS of Equation (10) at $z = mL + g/2$. Dot multiplying them by $\mathbf{e}_n$, and then integrating over $S_1 + S_2$ leads to

$$u_n = \rho_n + \chi_n + A_n e^{-j(\beta_n - k)g/2} + B_n e^{j(\beta_n + k)g/2}, \tag{12}$$

where

$$u_n = \int_{S_1} \mathbf{u} \cdot \mathbf{e}_n dS, \tag{13}$$

$$\chi_n = \int_{S_2} \nabla\chi \cdot \mathbf{e}_n dS, \tag{14}$$

$$\rho = \chi - \sigma, \tag{15}$$

$$\rho_n = \int_{S_1} \nabla\rho \cdot \mathbf{e}_n dS. \tag{16}$$

Similarly, by equating the RHS of Equation (5) and the RHS of Equation (11) at $z = mL - g/2$, dot multiplying them by $\mathbf{e}_n$, and integrating over $S_1 + S_2$ we get the following expression

$$v_n = \rho_n + \chi_n + A_n e^{-j(\beta_n - k)L} e^{j(\beta_n - k)g/2} + B_n e^{j(\beta_n + k)L} e^{-j(\beta_n + k)g/2}, \tag{17}$$

where

$$v_n = \int_{S_1} \mathbf{v} \cdot \mathbf{e}_n dS. \tag{18}$$

On the other hand, we equate Equation (8) and Equation (10) at $z = mL + g/2$, dot multiply them by $\mathbf{e}_\mu$, then integrate over S_1, and find that

$$u_\mu = C_\mu e^{-j(\beta_\mu - k)g/2} + D_\mu e^{j(\beta_\mu + k)g/2}, \tag{19}$$

where

$$u_\mu = \int_{S_1} \mathbf{u} \cdot \mathbf{e}_\mu dS. \tag{20}$$

Equating Equation (8) and Equation (11) at $z = mL - g/2$, dot multiplying them by $\mathbf{e}_\mu$, and then integrating over S_1 leads to

$$v_\mu = C_\mu e^{j(\beta_\mu - k)g/2} + D_\mu e^{-j(\beta_\mu + k)g/2}, \tag{21}$$

where

$$v_\mu = \int_{S_1} \mathbf{v} \cdot \mathbf{e}_\mu dS. \tag{22}$$

By solving Equation (12) and Equation (17) we get the following expressions for A_n and B_n in terms of u_n, v_n, ρ_n and χ_n. These expressions will be used later.

$$A_n = \frac{[u_n - (\rho_n + \chi_n)]e^{j\beta_n L}e^{-j(\beta_n+k)g/2} - [v_n - (\rho_n + \chi_n)]e^{-jkL}e^{j(\beta_n+k)g/2}}{2j \sin \beta_n (L-g)}, \tag{23}$$

$$B_n = -\frac{[u_n - (\rho_n + \chi_n)]e^{-j\beta_n L}e^{j(\beta_n-k)g/2} - [v_n - (\rho_n + \chi_n)]e^{-jkL}e^{-j(\beta_n-k)g/2}}{2j \sin \beta_n (L-g)}. \tag{24}$$

Similarly, solving Equation (19) and Equation (21) leads to expressions for C_μ and D_μ in terms of u_μ and v_μ.

$$C_\mu = -\frac{u_\mu e^{-j(\beta_\mu+k)g/2} - v_\mu e^{j(\beta_\mu+k)g/2}}{2j \sin \beta_\mu g}, \tag{25}$$

$$D_\mu = \frac{u_\mu e^{j(\beta_\mu-k)g/2} - v_\mu e^{-j(\beta_\mu-k)g/2}}{2j \sin \beta_\mu g}. \tag{26}$$

By matching transverse magnetic fields expressed by Equation (6) and Equation (9) at $z = mL + g/2$ we get a relation

$$\sum_n \mathbf{e}_n \frac{\lambda_n}{j \sin \beta_n (L-g)} \{[u_n - (\rho_n + \chi_n)] \cos \beta_n (L-g) - [v_n - (\rho_n + \chi_n)]e^{-jk(L-g)}\} + \nabla \rho = \sum_\mu \mathbf{e}_\mu \frac{\lambda_\mu}{j \sin \beta_\mu (L-g)} \{-u_\mu \cos \beta_\mu g + v_\mu e^{jkg}\}. \tag{27}$$

And matching Equation (6) and Equation (9) at $z = mL - g/2$ yields

$$\sum_n \mathbf{e}_n \frac{\lambda_n}{j \sin\beta_n(L-g)} \{[u_n - (\rho_n + \chi_n)]e^{jk(L-g)} - [v_n - (\rho_n + \chi_n)]\cos\beta_n(L-g)\} + \nabla\rho = \sum_\mu \mathbf{e}_\mu \frac{\lambda_\mu}{j \sin\beta_\mu g}\{-u_\mu e^{-jkg} + v_\mu \cos\beta_\mu g\}. \tag{28}$$

By subtracting Equation (28) from Equation (27) we get our first integral equation,

$$\mathbf{G}_1(\mathbf{r}) + \mathbf{G}_2(\mathbf{r}) = \int_{S_1} \overleftrightarrow{\mathbf{K}}{}_1^1(\mathbf{r},\mathbf{r}') \cdot \mathbf{u}(\mathbf{r}')dS' + \int_{S_1} \overleftrightarrow{\mathbf{K}}{}_2^1(\mathbf{r},\mathbf{r}') \cdot \mathbf{v}(\mathbf{r}')dS'. \tag{29}$$

Here,

$$\mathbf{G}_1(\mathbf{r}) = \sum_n \mathbf{e}_n(\mathbf{r}) \frac{\lambda_n(\rho_n + \chi_n)}{j \sin\beta_n(L-g)}[e^{jk(L-g)} - \cos\beta_n(L-g)] - \nabla\rho, \tag{30}$$

$$\mathbf{G}_2(\mathbf{r}) = \sum_n \mathbf{e}_n(\mathbf{r}) \frac{\lambda_n(\rho_n + \chi_n)}{j \sin\beta_n(L-g)}[e^{-jk(L-g)} - \cos\beta_n(L-g)] + \nabla\rho, \tag{31}$$

$$\overleftrightarrow{\mathbf{K}}{}_1^1(\mathbf{r},\mathbf{r}') = \sum_n \mathbf{e}_n(\mathbf{r})\mathbf{e}_n(\mathbf{r}') \frac{\lambda_n}{j \sin\beta_n(L-g)}[e^{jk(L-g)} - \cos\beta_n(L-g)] + \sum_\mu \mathbf{e}_\mu(\mathbf{r})\mathbf{e}_\mu(\mathbf{r}') \frac{\lambda_\mu}{j \sin\beta_\mu g}[e^{-jkg} - \cos\beta_\mu g], \tag{32}$$

$$\overleftrightarrow{\mathbf{K}}{}_2^1(\mathbf{r},\mathbf{r}') = \sum_n \mathbf{e}_n(\mathbf{r})\mathbf{e}_n(\mathbf{r}') \frac{\lambda_n}{j \sin\beta_n(L-g)}[e^{-jk(L-g)} - \cos\beta_n(L-g)] + \sum_\mu \mathbf{e}_\mu(\mathbf{r})\mathbf{e}_\mu(\mathbf{r}') \frac{\lambda_\mu}{j \sin\beta_\mu g}[e^{jkg} - \cos\beta_\mu g], \tag{33}$$

where $\overleftrightarrow{\mathbf{K}}{}_1^1(\mathbf{r},\mathbf{r}')$ and $\overleftrightarrow{\mathbf{K}}{}_2^1(\mathbf{r},\mathbf{r}')$ are integral kernels. Adding Equation (27) and Equation (28) leads to the second integral equation

$$\mathbf{G}_1(\mathbf{r})-\mathbf{G}_2(\mathbf{r})=\int_{S_1}\overleftrightarrow{\mathbf{K}}{}_1^2(\mathbf{r},\mathbf{r}')\cdot\mathbf{u}(\mathbf{r}')dS'-\int_{S_1}\overleftrightarrow{\mathbf{K}}{}_2^2(\mathbf{r},\mathbf{r}')\cdot\mathbf{v}(\mathbf{r}')dS', \tag{34}$$

where

$$\begin{aligned}\overleftrightarrow{\mathbf{K}}{}_1^2(\mathbf{r},\mathbf{r}')=&\sum_n\mathbf{e}_n(\mathbf{r})\mathbf{e}_n(\mathbf{r}')\frac{\lambda_n}{j\sin\beta_n(L-g)}[e^{jk(L-g)}+\cos\beta_n(L-g)]\\&+\sum_\mu\mathbf{e}_\mu(\mathbf{r})\mathbf{e}_\mu(\mathbf{r}')\frac{\lambda_\mu}{j\sin\beta_\mu g}[e^{-jkg}+\cos\beta_\mu g],\end{aligned} \tag{35}$$

$$\begin{aligned}\overleftrightarrow{\mathbf{K}}{}_2^2(\mathbf{r},\mathbf{r}')=&\sum_n\mathbf{e}_n(\mathbf{r})\mathbf{e}_n(\mathbf{r}')\frac{\lambda_n}{j\sin\beta_n(L-g)}[e^{-jk(L-g)}+\cos\beta_n(L-g)]\\&+\sum_\mu\mathbf{e}_\mu(\mathbf{r})\mathbf{e}_\mu(\mathbf{r}')\frac{\lambda_\mu}{j\sin\beta_\mu g}[e^{jkg}+\cos\beta_\mu g],\end{aligned} \tag{36}$$

are other two integral kernels.

These four integral kernels $\overleftrightarrow{\mathbf{K}}{}_1^1(\mathbf{r},\mathbf{r}')$, $\overleftrightarrow{\mathbf{K}}{}_2^1(\mathbf{r},\mathbf{r}')$, $\overleftrightarrow{\mathbf{K}}{}_1^2(\mathbf{r},\mathbf{r}')$ and $\overleftrightarrow{\mathbf{K}}{}_2^2(\mathbf{r},\mathbf{r}')$ are instrumental in the calculation which follows. It is easy to see that

$$\overleftrightarrow{\mathbf{K}}{}_1^1(\mathbf{r},\mathbf{r}')-\overleftrightarrow{\mathbf{K}}{}_2^1(\mathbf{r},\mathbf{r}')=\overleftrightarrow{\mathbf{K}}{}_1^2(\mathbf{r},\mathbf{r}')-\overleftrightarrow{\mathbf{K}}{}_2^2(\mathbf{r},\mathbf{r}'). \tag{37}$$

This relation is important in obtaining the variational form of the coupling impedance for the periodic structure of concern here.

3 COUPLING IMPEDANCE

The coupling impedance of the periodic structure we are studying is defined in terms of the surface integral,

$$Z(k)=Z_0W_0\int_{\text{on iris}}dS\,\mathbf{n}\cdot(\mathbf{E}_0^*\times Z_0\mathbf{H}), \tag{38}$$

where W_0 is a constant which differs for the longitudinal and transverse cases, and $\mathbf{n}$ is the unit inward normal on the iris surface. The integral in Equation (38) can be separated into two parts: $Z_1(k)$ which is the integral on both side walls and $Z_2(k)$ which is the integral on the surface of the iris hole.

$$Z_1(k) = Z_0 W_0 \int_{S_2} dS \Big\{ [\mathbf{E}_0^* \cdot (Z_0 \mathbf{H}_\perp \times \hat{\mathbf{z}})]_{z=mL-\frac{g}{2}} - [\mathbf{E}_0^* \cdot (Z_0 \mathbf{H}_\perp \times \hat{\mathbf{z}})]_{z=mL+\frac{g}{2}} \Big\}, \tag{39}$$

$$Z_2(k) = Z_0 W_0 \int_{S_h} dS [E_{0,\theta}^* Z_0 H_z]. \tag{40}$$

Here, S_h indicates the surface of the iris hole. By feeding the electromagnetic fields represented in Equation (1) and Equation (6) into the expression of $Z_1(k)$ in Equation (39) we get the impedance $Z_1(k)$ which is described in terms of coefficients A_n and B_n. Then we substitute A_n and B_n in Equation (23) and Equation (24) into this new expression of $Z_1(k)$ and finally get the expression for $Z_1(k)$ in terms of u_n, v_n, ρ_n and χ_n.

$$Z_1(k) = Z_0 W_0 |A_0|^2 \sum_n \frac{\lambda_n \chi_n}{j \sin \beta_n (L-g)} \times \{[u_n - (\rho_n + \chi_n)][e^{jk(L-g)} - \cos \beta_n (L-g)] + [v_n - (\rho_n + \chi_n][e^{-jk(L-g)} - \cos \beta_n (L-g)]\}. \tag{41}$$

In order to be able to calculate $Z_2(k)$, we need to derive H_z inside the iris hole from the transverse magnetic field $\mathbf{H}_\perp$ in Equation (9) and Maxwell equations, as we did earlier.[1] Since only TE modes contribute to H_z we do not need to consider TM modes in our calculation. The μ^{th} TE mode can be expressed in terms of the magnetic potential ψ_μ inside the iris hole as

$$\mathbf{e}_\mu = \mathbf{h}_\mu \times \hat{\mathbf{z}} = -\nabla \psi_\mu \times \hat{\mathbf{z}}. \tag{42}$$

Therefore, H_z can be written as

$$Z_0 H_z = -j A_0 \frac{e^{-jkmL}}{k} \sum_\mu^{TE} (k^2 - \beta_\mu^2) \psi_\mu [C_\mu e^{-j\beta_\mu (z-mL)} + D_\mu e^{j\beta_\mu (z-mL)}]. \tag{43}$$

It is obvious that ρ_μ vanishes for TM modes, but not for TE modes. By performing some algebra we conclude that

$$\rho_\mu = \oint d\theta \psi_\mu(b) \frac{\partial \chi}{\partial \theta}(b). \tag{44}$$

Substitution of $E^*_{0,\theta}$ and H_z into the integral expression for $Z_2(k)$ in Equation (40) leads to an expression for the impedance $Z_2(k)$ which is described in terms of the expansion coefficients C_μ and D_μ. After adopting the expressions in Equation (25), Equation (26) and Equation (44) for C_μ, D_μ and ρ_μ we finally obtain the expression for $Z_2(k)$ in terms of u_μ, v_μ and ρ_μ.

$$\begin{aligned} Z_2(k) = &- Z_0 W_0 |A_0|^2 \sum_\mu^{TE} \rho_\mu (u_\mu - v_\mu) \\ &+ Z_0 W_0 |A_0|^2 \sum_\mu^{TE} \lambda_\mu \rho_\mu (u_\mu - v_\mu e^{jkg}) \times \\ &e^{-jkg/2} \sin \frac{kg}{2} \cot \frac{\beta_\mu g}{2} \\ &+ j Z_0 W_0 |A_0|^2 \sum_\mu^{TE} \lambda_\mu \rho_\mu (u_\mu + v_\mu e^{jkg}) \times \\ &e^{-jkg/2} \cos \frac{kg}{2} \tan \frac{\beta_\mu g}{2}. \end{aligned} \tag{45}$$

On the other hand, if we add Equation (27), and Equation (28) multiplied by e^{jkg}, and dot multiply both sides of the new equation by $\nabla \rho$ and then integrate over S_1 we get the following result

$$\begin{aligned} &\sum_\mu^{TE} \lambda_\mu \rho_\mu (u_\mu - v_\mu e^{jkg}) j \cot \frac{\beta_\mu g}{2} \\ &= (1 + e^{jkg}) \int_{S_1} (\nabla \rho)^2 dS + \sum_n \frac{\lambda_n \rho_n}{j \sin \beta_n (L - g)} \times \\ &\{[u_n - (\rho_n + \chi_n)][\cos \beta_n (L - g) + e^{jkL}] \\ &- [v_n - (\rho_n + \chi_n)][e^{-jkL} + \cos \beta_n (L - g)] e^{jkg}\}. \end{aligned} \tag{46}$$

By subtracting Equation (28) multiplied by e^{jkg} from Equation (27) and dot multiplying both sides of the new equation by $\nabla\rho$ and then integrating over S_1 we obtain

$$\sum_{\mu}^{TE} \lambda_\mu \rho_\mu (u_\mu + v_\mu e^{jkg})(-j) \tan \frac{\beta_\mu g}{2}$$

$$= (1 - e^{jkg}) \int_{S_1} (\nabla\rho)^2 dS + \sum_n \frac{\lambda_n \rho_n}{j \sin \beta_n (L-g)} \times$$

$$\{[u_n - (\rho_n + \chi_n)][\cos \beta_n (L-g) e^{jkL}]$$

$$- [v_n - (\rho_n + \chi_n)][e^{-jkL} \cos \beta_n (L-g)] e^{jkg}\}. \quad (47)$$

By substituting Equation (46) and Equation (47) into Equation (45) we obtain a new expression of $Z_2(k)$ which will conveniently lead to the variational formulation for the total impedance.

$$Z_2(k) = Z_0 W_0 |A_0|^2 \sum_n \frac{\lambda_n \rho_n}{j \sin \beta_n (L-g)} \times$$

$$\{[u_n - (\rho_n + \chi_n)][e^{jk(L-g)} - \cos \beta_n (L-g)]$$

$$+ [v_n - (\rho_n + \chi_n)][e^{-jk(L-g)}$$

$$- \cos \beta_n (L-g)]\} - Z_0 W_0 |A_0|^2 \sum_{\mu}^{\mathrm{TE}} \rho_\mu (u_\mu - v_\mu). \quad (48)$$

Adding Equation (41) and Equation (48) yields the final expression for the total impedance of the periodic structure we have been studying. Our final form of the impedance consists of two parts: the explicit term, $G_0(k)$, and the variational term, $Z_{\mathrm{var}}(k)$.

$$Z(k) = G_0(k) + Z_{\mathrm{var}}(k). \quad (49)$$

Here, the explicit term, $G_0(k)$, turns out to be a sum over the indices of the normal modes in the pipe region.

$$G_0(k) = -2 Z_0 W_0 |A_0|^2 \sum_n \frac{\lambda_n (\rho_n + \chi_n)^2}{j \sin \beta_n (L-g)} [\cos k(L-g) - \cos \beta_n (L-g)]. \quad (50)$$

It is easy to show that $\rho_n + \chi_n$ vanishes for TE modes. Therefore, the sum is actually over TM cavity modes only. The second term $Z_{\text{var}}(k)$ is

$$Z_{\text{var}}(k) = Z_0 W_0 |A_0|^2 \left[\int_{S_1} \mathbf{G}_1 \cdot \mathbf{u} dS + \int_{S_1} \mathbf{G}_2 \cdot \mathbf{v} dS \right]. \tag{51}$$

Here, $\mathbf{G}_1$ and $\mathbf{G}_2$ are given in Equation (30) and Equation (31). We will construct a variational form for Equation (51) by regrouping the two parameter vector fields $\mathbf{u}$ and $\mathbf{v}$. Let us write

$$\mathbf{u} = \mathbf{U} + \mathbf{V}, \tag{52}$$

$$\mathbf{v} = \mathbf{U} - \mathbf{V}. \tag{53}$$

Substituting Equation (52) and Equation (53) into the brackets of the RHS of Equation (51) leads to

$$\int_{S_1} \mathbf{G}_1 \cdot \mathbf{u} dS + \int_{S_1} \mathbf{G}_2 \cdot \mathbf{v} dS = \int_{S_1} (\mathbf{G}_1 + \mathbf{G}_2) \cdot \mathbf{U} dS + \int_{S_1} (\mathbf{G}_1 - \mathbf{G}_2) \cdot \mathbf{V} dS. \tag{54}$$

By feeding Equation (29) and Equation (34) into Equation (54) we get

$$\begin{aligned} M &= \int_{S_1} (\mathbf{G}_1 + \mathbf{G}_2) \cdot \mathbf{U} dS + \int_{S_1} (\mathbf{G}_1 - \mathbf{G}_2) \cdot \mathbf{V} dS \\ &= \int_{S_1} dS \int_{S_1} dS' \mathbf{U} \cdot (\overleftrightarrow{\mathbf{K}}{}_1^1 + \overleftrightarrow{\mathbf{K}}{}_2^1) \cdot \mathbf{U} + \int_{S_1} dS \int_{S_1} dS' \mathbf{U} \cdot (\overleftrightarrow{\mathbf{K}}{}_1^1 - \overleftrightarrow{\mathbf{K}}{}_2^1) \cdot \mathbf{V} \\ &\quad + \int_{S_1} dS \int_{S_1} dS' \mathbf{V} \cdot (\overleftrightarrow{\mathbf{K}}{}_1^2 - \overleftrightarrow{\mathbf{K}}{}_2^2) \cdot \mathbf{U} \\ &\quad + \int_{S_1} dS \int_{S_1} dS' \mathbf{V} \cdot (\overleftrightarrow{\mathbf{K}}{}_1^2 + \overleftrightarrow{\mathbf{K}}{}_2^2) \cdot \mathbf{V}. \end{aligned} \tag{55}$$

We can therefore rewrite $Z_{\text{var}}(k)$ as

$$Z_{\text{var}}(k) = Z_0 W_0 |A_0|^2 \frac{\left[\int_{S_1} (\mathbf{G}_1 + \mathbf{G}_2) \cdot \mathbf{U} dS + \int_{S_1} (\mathbf{G}_1 - \mathbf{G}_2) \cdot \mathbf{V} dS \right]^2}{M}, \tag{56}$$

where M is the second form in Equation (55). If we ask that M be an extremum subject to the constraint

$$\int_{S_1} (\mathbf{G}_1 + \mathbf{G}_2) \cdot \mathbf{U} dS + \int_{S_1} (\mathbf{G}_1 - \mathbf{G}_2) \cdot \mathbf{V} dS = \text{ constant.} \tag{57}$$

we can use the Lagrange multiplier method to show that $\mathbf{U}$ and $\mathbf{V}$ must satisfy

$$\int_{S_1} (\overleftrightarrow{\mathbf{K}}_1^1 + \overleftrightarrow{\mathbf{K}}_2^1) \cdot \mathbf{U} dS' + \int_{S_1} (\overleftrightarrow{\mathbf{K}}_1^1 - \overleftrightarrow{\mathbf{K}}_2^1) \cdot \mathbf{V} dS' = \lambda(\mathbf{G}_1 + \mathbf{G}_2), \tag{58}$$

$$\int_{S_1} (\overleftrightarrow{\mathbf{K}}_1^2 - \overleftrightarrow{\mathbf{K}}_2^2) \cdot \mathbf{U} dS' + \int_{S_1} (\overleftrightarrow{\mathbf{K}}_1^2 + \overleftrightarrow{\mathbf{K}}_2^2) \cdot \mathbf{V} dS' = \lambda(\mathbf{G}_1 - \mathbf{G}_2), \tag{59}$$

Since these are, apart from a scaling constant, the same as the integral equation in Equations (29) and (34), and since Equation (56) is independent of any common scaling constant for $\mathbf{U}$ and $\mathbf{V}$, Z_{var} in Equation (56) is a variational form for the impedance $Z(k) - G_0(k)$.

4 REAL AND IMAGINARY PARTS OF THE IMPEDANCE: GENERAL OBSERVATIONS

Examination of Equation (50) and the results of Appendix A leads to the conclusion that the impedance is purely imaginary. This conclusion is clearly incorrect for frequencies above the pipe cutoff, particularly since we know that the real and imaginary parts are related by causality. What has happened is that the impedance has poles in the complex k plane just above the real axis and the real part is simply a sum of delta functions at the frequencies corresponding to these poles. The computation therefore yields a vanishing real part, except at the poles, where the numerical procedure is expected to fail for both the real and imaginary parts.

If the real part vanishes, except at isolated resonances, the Kramers-Kronig relation giving the imaginary part as an integral over the real part leads to the form

$$\frac{X_{\parallel}(k)}{Z_0} = \sum_n \frac{a_n k}{k_n^2 - k^2}, \tag{60}$$

for the imaginary part. All a_n's are positive to satisfy Foster's Reactance Theorem.[6] If we now move the poles to a position slightly above the real axis, we can write, for very small ϵ,

$$\frac{Z_{\parallel}(k)}{Z_0} = \sum_n \frac{ja_n k}{k_n^2 - k^2 + j\epsilon} \tag{61}$$

Thus, using $\lim_{\epsilon \to 0}[\epsilon/(\epsilon^2 + x^2)] = \pi^{-1}\delta(x)$, we have

$$\frac{R_{\parallel}(k)}{Z_0} = \lim_{\epsilon \to 0} \sum_n \frac{a_n k \epsilon}{(k_n^2 - k^2)^2 + \epsilon^2} = \frac{1}{\pi} \sum_n a_n k_n \delta(k^2 - k_n^2). \tag{62}$$

We can therefore use the computed behavior of $X_{\parallel}(k)$ near each resonance at $k = k_n$ to determine a_n by fitting $Z_0/X_{\parallel}(k)$ as a linear function of $k - k_n$ near $k = k_n$, and from these a_n's obtain the real part of the impedance as a sum of delta functions with specified coefficients. Clearly these delta functions will be broadened if the wall conductivity is finite.

It appears that the resonances at $k = k_n$ correspond to the frequencies at which propagation of azimuthally symmetric modes through the structure produces a phase advance of kL per period of length L, in order to be in synchronism with the particle moving with velocity c. This is confirmed from the dispersion curves calculated with our geometry, using the program KN7C.[3]

The total impedance is therefore

$$\frac{Z_{\parallel}(k)}{Z_0} = \frac{1}{\pi} \sum_n a_n k_n \delta(k^2 - k_n^2) + jk \sum_n \frac{a_n}{k_n^2 - k^2}, \tag{63}$$

where the sum is over all values of n corresponding to positive k_n. Clearly $Z_{\parallel}^*(k) = Z_{\parallel}(-k)$, as required.

A similar situation exists for the transverse impedance, where we find

$$\frac{Z_{\perp}(k)}{Z_0} = \frac{k}{\pi} \sum_n b_n \delta(k^2 - k_n^2) + j \sum_n \frac{b_n k_n}{k_n^2 - k^2}. \tag{64}$$

This time we satisfy $Z_{\perp}^*(k) = -Z_{\perp}(-k)$, and the location of the poles corresponds to the propagation of modes proportional to $\cos\theta$, $\sin\theta$ with a phase advance of kL per period.

5 NUMERICAL RESULTS FOR CYLINDRICAL PIPE WITH CIRCULAR IRISES

In our numerical implementation, we choose cylindrical pipe and circular irises as our example. The radius of pipe and the radius of iris hole are a and b respectively. In the longitudinal case, both source potentials $\chi(r)$ and $\sigma(r)$ are equal to $-\ln(r)$. The constant coefficient is $W_0|A_0|^2 = 1/2\pi^2$. TE modes do not contribute to the longitudinal impedance. The normalized TM modes are $\mathbf{e}_n(r) = -\nabla\phi_n(r)$ and $\mathbf{e}_{\mu}(r) = -\nabla\phi_{\mu}(r)$. The potentials are

$$\phi_n(r) = \frac{J_0(p_n r/a)}{\sqrt{\pi}\, p_n J_1(p_n)}, \tag{65}$$

$$\phi_\mu(r) = \frac{J_0(p_\mu r/b)}{\sqrt{\pi}\, p_\mu J_1(p_\mu)}. \tag{66}$$

where $J_i(s)$ is the Bessel function of i$^{\text{th}}$ order, p_j is the j$^{\text{th}}$ zero of $J_0(s)$.

In the transverse case, the source potential $\chi(r, \theta)$ is $(r^2 - a^2)\cos\theta/r$, while $\sigma(r, \theta)$ equals $(r^2 - b^2)\cos\theta/r$. The constant coefficient $W_0|A_0|^2 = 1/2\pi^2 k$. Both TM and TE modes contribute to the transverse impedance. The normalized TM modes are $\mathbf{e}_n(r, \theta) = -\nabla\phi_n(r, \theta)$ and $\mathbf{e}_\mu(r, \theta) = -\nabla\phi_\mu(r, \theta)$, while the normalized TE modes are $\mathbf{e}_n(r, \theta) = -\nabla\psi_n(r, \theta) \times \hat{\mathbf{z}}$ and $\mathbf{e}_\mu(r, \theta) = -\nabla\psi_\mu(r, \theta) \times \hat{\mathbf{z}}$. The field potentials are

$$\phi_n(r) = \sqrt{\frac{2}{\pi}} \frac{J_1(p_n r/a)}{p_n J_0(p_n)} \cos\theta, \tag{67}$$

$$\psi_n(r) = \sqrt{\frac{2}{\pi}} \frac{J_0(q_n r/a)}{\sqrt{q_n^2 - 1} J_1(q_n)} \sin\theta, \tag{68}$$

$$\phi_\mu(r) = \sqrt{\frac{2}{\pi}} \frac{J_1(p_\mu r/b)}{p_\mu J_0(p_\mu)} \cos\theta, \tag{69}$$

$$\psi_\mu(r) = \sqrt{\frac{2}{\pi}} \frac{J_0(q_\mu r/b)}{\sqrt{q_\mu^2 - 1} J_1(q_\mu)} \sin\theta, \tag{70}$$

where p_j is the j$^{\text{th}}$ zero of $J_1(s)$, and q_j is the j$^{\text{th}}$ zero of $dJ_1(s)/ds$.

In both the longitudinal and transverse cases, the propagation constants can be written as

$$\beta_n = \begin{cases} \sqrt{k^2 - p_n^2/a^2} = -j\sqrt{p_n^2/a^2 - k^2} \\ \sqrt{k^2 - q_n^2/a^2} = -j\sqrt{q_n^2/a^2 - k^2} \end{cases}, \tag{71}$$

$$\beta_\mu = \begin{cases} \sqrt{k^2 - p_\mu^2/b^2} = -j\sqrt{p_\mu^2/b^2 - k^2} \\ \sqrt{k^2 - q_\mu^2/b^2} = -j\sqrt{q_\mu^2/b^2 - k^2} \end{cases}. \tag{72}$$

Computer codes were written based on the formulas obtained in previous sections to compute the longitudinal and transverse impedances. It turns out that the impedances are purely imaginary as predicted in Section 4. The missing real part of the impedance is retrieved by using causality. By calculating for a wide range of structure parameters, the codes show very good convergence properties. For b/a greater than 0.1, L/a between 0.5 and 2.0, and g/a less than 1.0, the number of modes needed for good convergence in the iris hole is around 10 and the number of modes needed in the pipe region is under 100. The numerical results are accurate to four significant figures, as determined by varying the number of modes used. In fact, our earlier experience with the variational approach[1] showed that it gave more accurate results with fewer modes than an earlier non-variational result with a much greater number of modes.

Figures 1, 2, 3 and 4 present the imaginary and real parts of longitudinal and transverse impedances for $b/a = 0.45$, $L/a = 1.1$, $g/a = 0.35$. There is a series of isolated narrow resonances in the calculated imaginary part of impedance. From there we have successfully retrieved the real part of impedance which turns out to be a sum of delta functions with specified coefficients as described in Equations (63) and (64). These coefficients are obtained by fitting the inverse of the imaginary part to a power series in the vicinity of each resonance. Again we believe these coefficients are accurate to 4 or 5 decimals in the loss factor. The positions of the resonances are the intersections of dispersion curves with the light line. These are the resonant modes propagating with the velocity of light in the periodic structure. The resonant modes and loss factors obtained from our calculation agree well with those from the well known computer codes KN7C[3] and TRANSVRS,[7] which are presented in Tables 1 and 2,[8] but we have no way to estimate their accuracy in the few cases where our results differ.

6 SUMMARY

We constructed a variational form for the longitudinal and transverse impedances of periodic irises in a beam pipe. The numerical implementation for a cylindrical pipe with circular irises shows very good convergence and accuracy properties. For b/a greater than 0.1, L/a between 0.5 and 2.0, and g/a less than 1.0, the number of modes needed for good convergence in the iris hole is around 10 and the number of modes needed in the pipe region is under 100. The numerical results are accurate to four significant figures. The numerically calculated impedance is imaginary, except for isolated narrow resonances corresponding to modes propagating with the velocity of light. The real part of impedance is obtained by using causality. The resonances and loss factors obtained from the numerical calculation agree well with those from codes KN7C[3] and TRANSVRS.[7]

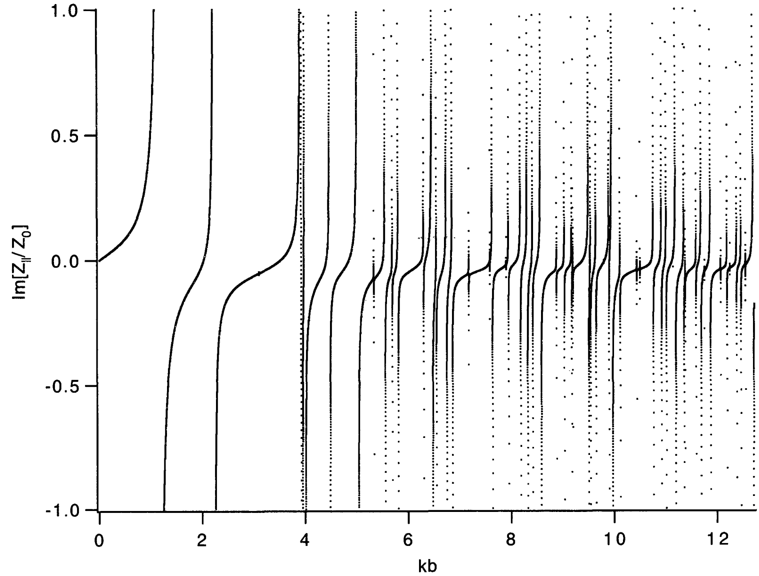

FIGURE 1: Imaginary part of longitudinal impedance ($b/a = 0.45$, $L/a = 1.1$, $g/a = 0.35$).

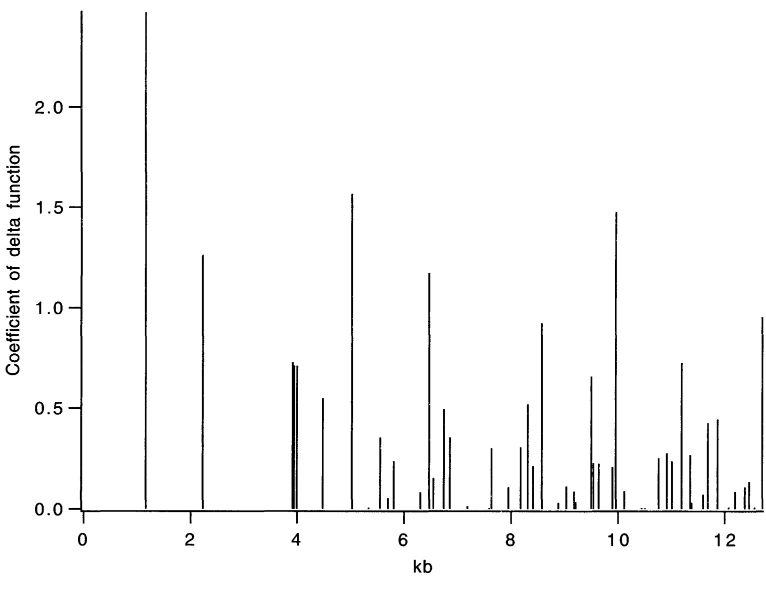

FIGURE 2: Real part of longitudinal impedance ($b/a = 0.45$, $L/a = 1.1$, $g/a = 0.35$).

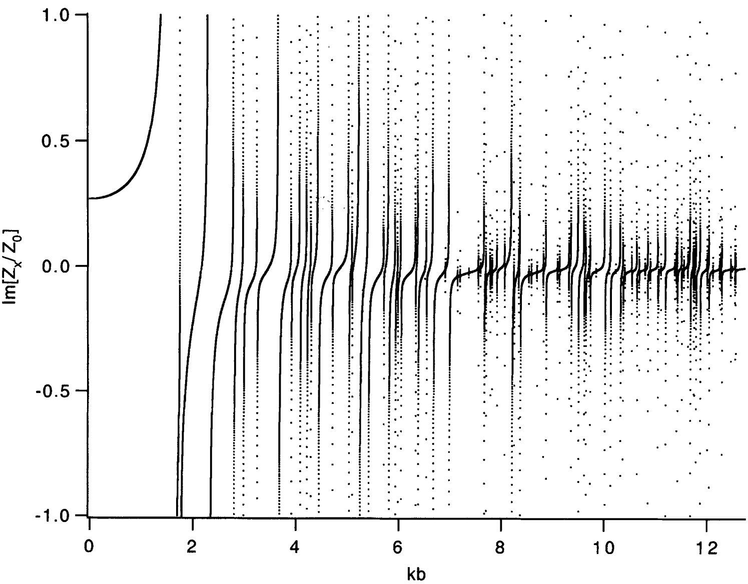

FIGURE 3: Imaginary part of transverse impedance ($b/a = 0.45$, $L/a = 1.1$, $g/a = 0.35$).

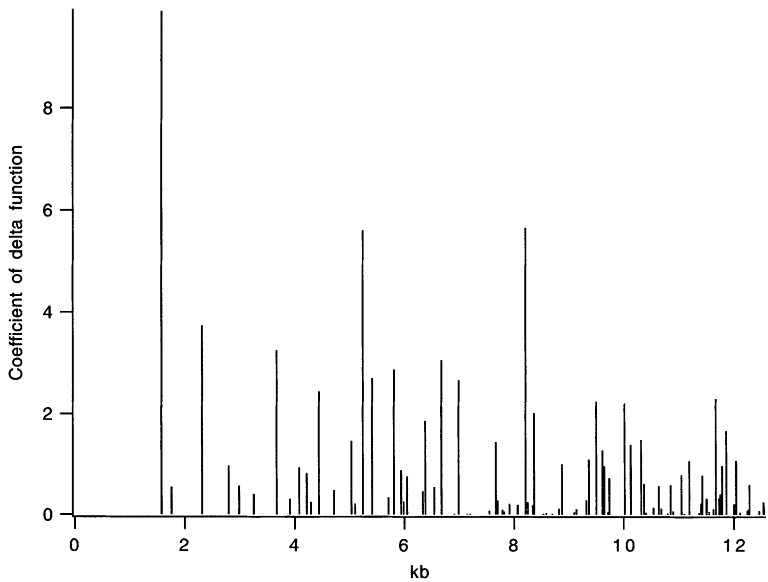

FIGURE 4: Real part of transverse impedance ($b/a = 0.45$, $L/a = 1.1$, $g/a = 0.35$).

TABLE 1: Resonances and loss factors of longitudinal impedance (b/a=0.45, L/a=1.1, g/a=0.35).

$k(cm^{-1})$		$kloss(V/pc)$	
KN7C	This Work	KN7C	This Work
2.581861	2.580688	2.102369E+00	2.125355E+00
4.961226	4.960281	3.036148E−01	5.653804E−01
5.492259	5.492233	4.480160E−06	6.866231E−06
6.904270	6.903624	1.744264E−05	2.389725E−05
8.709290	8.705066	2.009352E−01	1.854692E−01
8.758570	8.756767	2.025505E−01	1.803803E−01
8.886603	8.884985	1.625225E−01	1.778768E−01
9.957987	9.956777	1.394129E−01	1.223344E−01
11.16609	11.16232	3.032836E−01	3.115446E−01
11.85667	11.85651	1.386558E−03	1.395643E−03
12.34160	12.34116	7.549676E−02	6.368927E−02
12.65686	12.65615	1.099255E−02	9.395803E−03
12.91274	12.91212	3.696359E−02	4.090822E−02
14.01035	14.00670	1.071517E−02	1.336009E−02
14.37593	14.37306	1.723502E−01	1.809764E−01
14.55714	14.55551	2.030024E−02	2.326244E−02
14.99183	14.98819	6.012031E−02	7.348540E−02
15.24086	15.23880	7.112018E−02	5.168645E−02
15.95930	15.95784	2.426895E−03	2.061734E−03
16.87086	16.87078	5.337740E−04	5.409835E−04
16.96928	16.96881	3.935382E−02	3.942144E−02
17.57352	17.57260	1.441660E−04	1.231804E−04
17.67125	17.67100	1.329100E−02	1.382576E−02
18.18757	18.18502	3.538040E−02	3.734784E−02
18.48816	18.48700	6.999585E−02	6.230707E−02
18.71464	18.71164	2.304351E−02	2.531616E−02
19.07119	19.06647	7.361748E−02	1.071663E−01
19.74218	19.74198	3.863001E−03	3.534208E−03
20.08350	20.08145	1.250815E−02	1.236702E−02
20.40175	20.39608	7.888159E−03	9.609815E−03
20.45182	20.45091	5.871262E−03	3.828672E−03
21.12757	21.12571	5.383233E−02	6.890874E−02
21.21161	21.20809	2.546757E−02	2.378598E−02
21.44683	21.44576	2.305657E−02	2.317151E−02
21.79804	21.79620	1.432656E−05	1.055576E−05
22.01008	22.00839	2.380975E−02	2.106702E−02
22.15308	22.14706	1.046664E−01	1.477927E−01

TABLE 1: Continued.

$k(cm^{-1})$		$kloss(V/pc)$	
KN7C	This Work	KN7C	This Work
22.49162	22.48976	1.106724E−02	8.824543E−03
23.21233	23.21186	7.255406E−04	6.659727E−04
23.34886	23.34900	5.380351E−04	3.451418E−04
23.92931	23.92443	2.201252E−02	2.341916E−02
24.27843	24.27693	3.152963E−02	2.529073E−02
24.48221	24.47857	1.886040E−02	2.147969E−02
24.78022	24.77985	8.760262E−06	4.732936E−05
24.89037	24.88193	6.990967E−02	6.467110E−02
25.24489	25.24470	1.999847E−02	2.359107E−02
25.30306	25.30202	2.575565E−03	2.769796E−03
25.77722	25.76662	6.404670E−03	6.154389E−03
25.98125	25.98117	4.343236E−02	3.644507E−02
26.12604	26.12606	1.400007E−04	1.399280E−04
26.38547	26.38403	4.359393E−02	3.732571E−02
26.82733	26.82592	6.248882E−04	6.783228E−04
27.10509	27.10017	9.431480E−03	7.098141E−03
27.23079	27.23013	7.374468E−05	7.454248E−05
27.51533	27.51378	8.451375E−03	8.847252E−03
27.70673	27.70251	9.924205E−03	1.085202E−02
27.89819	27.89690	8.770565E−04	7.196698E−04
28.23482	28.23032	5.809697E−02	7.466184E−02

Acknowledgements

We are grateful to Dr. Karl L. Bane for providing the output of KN7C and TRANSVRS for our structure.

References

[1] H. Okamoto, S. Jiang and R. L. Gluckstern, *Phys. Rev. E* **50**, 1501 (1994).
[2] G. Dôme, E. Gianfelice, L. Palumbo, V. G. Vaccaro, and L. Verolino, *Nouvo Cimento A*, **104**, 1241 (1991).
[3] E. Keil, *Nucl. Instr. and Method* **100**, 419 (1972).
[4] E. Keil and B. Zotter, *Particle Accelerators* **3**, 11 (1972).
[5] G. Dôme, L. Palumbo, V.G. Vaccaro and L. Verolino, *Particle Accelerators*, **36** 161 (1991).
[6] E.A. Guillemin, *Communication Networks* (John Wiley & Sons, Inc., New York, 1931).
[7] K. Bane and B. Zotter, in Proceedings of the 11th International Conference on High Energy Accelerators, CERN (Birhäuser Verlag, Basel, 1980), p. 581.
[8] The vertical axis is the coefficient of the delta function in Eq. (4.3).

TABLE 2: Resonances and loss factors of transverse impedance (b/a=0.45, L/a=1.1, g/a=0.35).

$k(cm^{-1})$		$kloss(V/pc)$	
TRANSVRS	This Work	TRANSVRS	This Work
3.489852	3.489900	2.934492E+00	2.726712E+00
3.904021	3.905235	1.892190E−01	1.349643E−01
5.140928	5.139610	7.196953E−01	6.988519E−01
6.210159	6.210570	2.096863E−01	1.507692E−01
6.627860	6.628316	9.560569E−02	8.299518E−02
7.220360	7.218894	5.299862E−02	5.459084E−02
8.155369	8.153459	3.886702E−01	3.833443E−01
8.695464	8.696415	3.993099E−02	3.473799E−02
9.072788	9.072008	1.339229E−01	9.930918E−02
9.367758	9.370076	8.395114E−02	8.497068E−02
9.539883	9.542383	3.107584E−02	2.584012E−02
9.871684	9.869013	2.894455E−01	2.386512E−01
10.47332	10.47269	4.635401E−02	4.493226E−02
11.18601	11.18451	1.027246E−01	1.262097E−01
11.32649	11.32775	1.734654E−02	1.864130E−02
11.64974	11.64944	4.901797E−01	4.635592E−01
11.78998	11.79407	9.746761E−05	1.496705E−04
12.03382	12.03216	2.508256E−01	2.160359E−01
12.69608	12.69838	2.630085E−02	2.630127E−02
12.91728	12.91678	2.158531E−01	2.140696E−01
13.19840	13.20051	8.389785E−02	6.455673E−02
13.30195	13.30297	2.184627E−02	1.899008E−02
13.44864	13.44485	5.815653E−02	5.477051E−02
14.07997	14.08018	2.835567E−02	3.199006E−02
14.18994	14.18490	1.328887E−01	1.262955E−01
14.48289	14.48298	9.020805E−05	8.752686E−05
14.54447	14.54482	5.256668E−02	3.641890E−02
14.84243	14.84160	2.244227E−01	1.985304E−01
15.35473	15.35674	1.150722E−03	9.274188E−04
15.53631	15.53084	1.710797E−01	1.649242E−01

APPENDIX A

If we expand $\mathbf{U}$ and $\mathbf{V}$ in terms of $\mathbf{e}_\mu$, we may express $Z_{\rm var}(k)$ as

$$Z_{\rm var}(k) = Z_0 W_0 |A_0|^2 \frac{\left(\sum_\alpha C_\alpha\right)^2}{\sum_\alpha \sum_{\alpha'} C_\alpha P_{\alpha\alpha'} C_{\alpha'}}, \tag{73}$$

where

$$(C_\alpha) = (C_{\mu_1}, C_{\mu_2}), \tag{74}$$

$$\int_{S_1} (\mathbf{G}_1 + \mathbf{G}_2) \cdot \mathbf{U} dS + \int_{S_1} (\mathbf{G}_1 - \mathbf{G}_2) \cdot \mathbf{V} dS$$
$$= \sum_{\mu_1} C_{\mu_1} + \sum_{\mu_2} C_{\mu_2}, \tag{75}$$

$$(P_{\alpha\alpha'}) = \begin{pmatrix} P_{\mu_1,\mu_1'}, & P_{\mu_1,\mu_2'} \\ P_{\mu_2,\mu_1'}, & P_{\mu_2,\mu_2'} \end{pmatrix}, \tag{76}$$

$$\int_{S_1} dS \int_{S_1} dS' \mathbf{U} \cdot (\overleftrightarrow{\mathbf{K}}_1^1 + \overleftrightarrow{\mathbf{K}}_2^1) \cdot \mathbf{U} + \int_{S_1} dS \int_{S_1} dS' \mathbf{U} \cdot (\overleftrightarrow{\mathbf{K}}_1^1 - \overleftrightarrow{\mathbf{K}}_2^1) \cdot \mathbf{V}$$
$$+ \int_{S_1} dS \int_{S_1} dS' \mathbf{V} \cdot (\overleftrightarrow{\mathbf{K}}_1^2 - \overleftrightarrow{\mathbf{K}}_2^2) \cdot \mathbf{U} + \int_{S_1} dS \int_{S_1} dS' \mathbf{V} \cdot (\overleftrightarrow{\mathbf{K}}_1^2 + \overleftrightarrow{\mathbf{K}}_2^2) \cdot \mathbf{v}$$
$$= \sum_{\mu_1} \sum_{\mu_1'} C_{\mu_1} P_{\mu_1\mu_1'} C_{\mu_1'} + \sum_{\mu_1} \sum_{\mu_2'} C_{\mu_1} P_{\mu_1\mu_2'} C_{\mu_2'}$$
$$+ \sum_{\mu_2} \sum_{\mu_1'} C_{\mu_2} P_{\mu_2\mu_1'} C_{\mu_1'} + \sum_{\mu_2} \sum_{\mu_2'} C_{\mu_2} P_{\mu_2\mu_2'} C_{\mu_2'}. \tag{77}$$

By minimizing Equation (A1), we get $Z_{\text{var}}(k)$ in the form of sum over all elements of the reciprocal of matrix $(P_{\alpha\alpha'})$:

$$Z_{\text{var}}(k) = Z_0 W_0 |A_0|^2 \sum_{\alpha} \sum_{\alpha'} P_{\alpha\alpha'}^{-1}. \tag{78}$$

Next, we examine $P_{\alpha\alpha'}$ in detail. The explicit form of $\mathbf{G}_1 + \mathbf{G}_2$ is purely imaginary, while the explicit form of $\mathbf{G}_1 - \mathbf{G}_2$ is real. On the other hand, $\overleftrightarrow{\mathbf{K}}_1^1 + \overleftrightarrow{\mathbf{K}}_2^1$ is imaginary, $\overleftrightarrow{\mathbf{K}}_1^1 - \overleftrightarrow{\mathbf{K}}_2^1$ and $\overleftrightarrow{\mathbf{K}}_1^2 - \overleftrightarrow{\mathbf{K}}_2^2$ (they are equal) are real, and $\overleftrightarrow{\mathbf{K}}_1^2 + \overleftrightarrow{\mathbf{K}}_2^2$ is purely imaginary. All those lead to the fact that all elements of matrix are imaginary. Finally, we find that $Z_{\text{var}}(k)$ is purely imaginary.